Published in final edited form as:
*Drug Dev Res*. 2014 May ; 75(3): 172–188. doi:10.1002/ddr.21169.

# Uncovering Cryptic Glycan Markers in Multiple Sclerosis (MS) and Experimental Autoimmune Encephalomyelitis (EAE)

**Denong Wang**[1,*], **Roopa Bhat**[2], **Raymond A. Sobel**[3], **Wei Huang**[4], **Lai-Xi Wang**[4], **Tomas Olsson**[5], and **Lawrence Steinman**[2]

[1]Tumor Glycomics Laboratory, SRI International Biosciences Division, Menlo Park, CA 94025, USA

[2]Department of Neurology and Neurological Sciences, Stanford University School of Medicine, Stanford, CA 94305, USA

[3]Department of Pathology, Stanford University School of Medicine, Stanford, CA 94305, USA

[4]Institute of Human Virology, Department of Biochemistry & Molecular Biology, University of Maryland School of Medicine, Baltimore, MD 21201, USA

[5]Department of Clinical Neuroscience, Karolinska Institute, Stockholm, 171 76, Sweden

## Abstract

| Strategy, Management and Health Policy | | | | |
|---|---|---|---|---|
| Enabling Technology, Genomics, Proteomics | Preclinical Research | Preclinical Development Toxicology, Formulation Drug Delivery, Pharmacokinetics | Clinical Development Phases I-III Regulatory, Quality, Manufacturing | Postmarketing Phase IV |

Using an integrated antigen microarray approach, we observed epitope-spreading of autoantibody responses to a variety of antigenic structures in the cerebrospinal fluid (CSF) of patients with multiple sclerosis (MS) and in the serum of mice with experimental autoimmune encephalomyelitis (EAE). These included previously described protein- and lipid-based antigenic targets and newly discovered autoimmunogenic sugar moieties, notably, autoantibodies specific for the oligomannoses in both MS patient CSF and the sera of mice with EAE. These glycans are often masked by other sugar moieties and belong to a class of cryptic autoantigens. We further determined that these targets are highly expressed on multiple cell types in MS and EAE lesions. Co-immunization of SJL/J mice with a Man9-KLH conjugate at the time of EAE induction elicited highly significant levels of anti-Man9-cluster autoantibodies. Nevertheless, this anti-glycan autoantibody response was associated with a significantly reduced clinical severity of EAE.



*Correspondence to: Denong Wang, Tumor Glycomics Laboratory, SRI International Biosciences Division, 333 Ravenswood Avenue, Menlo Park, CA 94025, USA. denong.wang@sri.com.

The potential of these cryptic glycan markers and targeting antibodies for diagnostic and therapeutic interventions of neurological disorders has yet to be explored.

**Keywords**

glycomics; biomarkers; multiple sclerosis; encephalomyelitis; cryptic glycans; cerebrospinal fluid; autoantibodies

## INTRODUCTION

Multiple sclerosis (MS) is a complex neurological disorder in which an adaptive autoimmune response is thought to target myelin sheath in the central nervous system (CNS). Pathologically, there is inflammation in the CNS white matter with the infiltration of multiple immune cells, including T and B cells, macrophages and other inflammatory cells. Autoreactive T cells are believed to be important in the pathogenesis of MS lesions and in an animal model of MS, experimental autoimmune encephalomyelitis (EAE) [Lehmann et al., 1992; McRae et al., 1995; Yu et al., 1996a, 1996b]. Clonal expansion of B cells in brain tissue and the presence of oligoclonal immunoglobulins in the CSF of patients with MS are also hallmarks of the disease [Kabat et al., 1948, 1951; Steinman, 1996; Genain et al., 1999; Raine et al., 1999; Hueber et al., 2002].

Evaluation of autoantibodies in autoimmune diseases has been enabled by development of new technologies, e.g., microarray-based large-scale auto-antibody profiling [Robinson et al., 2002, 2003; Wang et al., 2002; Kanter et al., 2006; Beyer et al., 2012]. Robinson et al. developed “myelin proteome” microarrays to profile the evolution of autoantibody responses in an EAE model [Robinson et al., 2003] and found that the diversity of autoantibody responses increased as the disease evolved from acute to chronic relapsing EAE. Chronic EAE was associated with extensive intra- and intermolecular epitope spreading of autoreactive B-cell responses. Using human recombinant protein microarrays to examine auto-antibody profiles in the CSF of patients with relapsing-remitting MS (RRMS) led to the identification of a panel of proteins as possible differentiators between RRMS and other neurological diseases (OND) that warranted further investigation [Beyer et al., 2012].

Kanter et al. developed lipid arrays to monitor autoantibody responses against lipids present in the myelin sheath, including ganglioside, sulfatide, cerebroside, sphingomyelin, and total brain lipid fractions [Kanter et al., 2006]. This technology was applied to monitor lipid-specific antibody responses in CSF samples from individuals with MS and controls [Kanter et al., 2006; Ho et al., 2012]. These studies showed lipid-specific antibodies against sulfatide, sphingomyelin, and oxidized lipids in the CSF of MS patients. Sulfatide-specific antibodies were also detected in SJL/J mice with acute EAE. They further demonstrated that immunization of mice with sulfatide plus myelin peptide produced a more severe disease course of EAE, and administration of sulfatide-specific antibody exacerbated EAE. Thus, autoimmune responses to sulfatide and other lipids are present in individuals with MS and in EAE and may contribute to the pathogenesis of autoimmune demyelination.

Carbohydrates represent another class of antigenic structures with unique immunological properties [Wang and Kabat, 1996; Wang, 2004]. In brain, the myelin sheath and other tissues contain numerous sugar moieties, either in the form of glycolipids or as glycoproteins. Expression of brain carbohydrate, including mannosyl glycans, can be developmentally and/or differentially regulated [Schachter, 1991; Yuen et al., 1997; Chai et al., 1999a, 1999b; Michele and Campbell, 2003; Breloy et al., 2012a, 2012b; Pacharra et al., 2012]. Some carbohydrates that exist intracellularly as part of the process of protein glycosylation are masked by other sugar moieties when the mature glycoproteins are released extracellularly [Brooks et al., 2002]. Such "cryptic" carbohydrates are, however, potentially immunogenic [Calarese et al., 2003; Wang and Lu, 2004; Newsom-Davis et al., 2009; Walker et al., 2011]. For example, HIV-1 virions [Calarese et al., 2003; Walker et al., 2011] and certain tumors [Newsom-Davis et al., 2009; Wang, 2012b; Wang et al., 2013] abnormally express N-glycan high-mannose (Man9) clusters. HIV-infected subjects [Trkola et al., 1996; Walker et al., 2011] and some cancer patients [Wang, 2012b; Wang et al., 2013] develop anti-oligomannose autoantibody responses. These observations prompted us to ask whether MS/EAE-associated autoantibody responses can also target this class of cryptic autoantigens.

We have established a versatile bioarray platform to integrate the protein-, lipid-, and carbohydrate-based microarrays in order to facilitate identification of autoimmune targets in autoimmune diseases. In essence, we have demonstrated a practical approach to constructing antigen microarrays, with immobilization of carbohydrate, lipids/liposomes, and protein molecules on nitrocellulose-coated microglass slides [Wang et al., 2002, 2005; Wang, 2003; Wang and Lu, 2004]. This bioarray platform was used to display autoantigens of diverse molecular composition including proteins and peptides of myelin sheath, liposomes of distinct lipid composition, and carbohydrate antigens that display a number of "cryptic" glycoepitopes [Wang and Lu, 2004; Newsom-Davis et al., 2009; Wang, 2012b; Wang et al., 2013]. This bioarray platform supports quantitative measurement of the relative antibody reactivities (RAR) over a large-panel of antigens. Thus, it is technically suitable for monitoring the antigenic epitope-spreading of an autoimmune response in EAE and MS.

## METHODS AND MATERIALS

### Liposome Preparation

Methods of sonication (sonic energy) and extrusion (mechanical energy) used to produce liposomes were as described [Wang et al., 2005]. Two types of liposomes, *homo*- and *hetero*-liposomes, were used in this study. The former were produced via a single lipid preparation, e.g., phosphatidylcholine (PTC), cerebroside, and sulfatide. The latter contained two different lipid molecules with PTC as the support to display other lipid/glycolipid in desired ratios or epitope densities. For example, the *hetero*-liposome of sulfatide (Antigen ID, 30$^{\#}$) is composed of sulfatide and PTC at a ratio of 1:10 (wt/wt), i.e., 0.2 mg sulfatide and 2.0 mg PTC per ml of liposome suspension in saline. Compositions of all liposome preparations are given in Table 1.

### Printing Protein, Carbohydrate, and Lipid/Liposome Microarrays

A high-precision microarray robot (PIXSYS 5500C, Cartesian Technologies, Irvine, CA) was used to spot antigen preparations onto glass slides pre-coated with nitrocellulose polymer (FAST Slides; Schleicher & Schuell, Keene, NH) as described [Wang, 2012a]. The antigen preparations applied include proteins/peptides, carbohydrates, and liposomes of various composition (Table 1). Proteins and carbohydrates were dissolved in phosphate-buffered saline (PBS; pH 7.4) and saline (0.9% NaCl), respectively. Liposome preparations were suspended in saline (0.9% NaCl) at the concentrations specified (Table 1) and were printed in triplicate with spot sizes of ~150 μm and at 375 μm intervals, center to center. The printed microarrays were air-dried and stored at room temperature (RT) without desiccant before application.

### Staining and Scanning of Microarrays

Immediately before use, the printed microarrays were rinsed with PBS, pH 7.4, with 0.05% (vol/vol) Tween 20 and then blocked by incubating the slides in 1% (wt/vol) bovine serum albumin (BSA) in PBS containing 0.05% (wt/vol) $NaN_3$ at RT for 30 min. They were then incubated at RT with antibodies at an indicated titration in 1% (wt/vol) BSA in PBS containing 0.05% (wt/vol) $NaN_3$ and 0.05% (vol/vol) Tween 20. The secondary antibodies or streptavidin conjugates applied for microarray staining are specified in the figure legends. The stained slides were rinsed five times with PBS with 0.05% (vol/vol) Tween 20, air-dried at RT, and then scanned for fluorescent signals using a ScanArray5000A Microarray Scanner (PerkinElmer Life Science, Boston, MA) following the manufacturer's manual.

### Examination of Presence of Antigens on Array and Their Antigenic Determinants or Epitopes

It was essential to assess whether the proteins, synthetic peptides, and carbohydrates were successfully "printed" and whether desired epitopes or antigenic determinants were preserved on the chips. A practical approach was to incubate the printed microarrays with antibodies, receptors, or lectins known to react with the printed substance. As illustrated in Figure 1, we examined preservation of *Galanthus nivalis agglutinin* (GNA)-specific glyco-epitopes (Fig. 1A–C) or 2G12-specific glyco-epitopes (Fig. 1A, B, and D) by staining the spotted antigen arrays using corresponding probes. This demonstrated that the GNA-epitopes were presented by three glyco-conjugates, i.e., Man9-cluster ($4^{\#}$), M9_2G12-cluster ($3^{\#}$), and Man5–9 RB ($1^{\#}$). In contrast, 2G12-glyco-epitopes were well-preserved only by one of the three, i.e., M9_2G12-cluster ($3^{\#}$), in this microarray substrate.

### Microarray Data-Processing, Standardization, and Statistical Analysis

Fluorescence intensity values for each array spot and its background were calculated using ScanArray Express software. SAS Institute's JMP-Genomics software package (http://www.jmp.com/) (Cary, NC) was used for microarray data standardization and statistical analysis. In Figure 1, microarray detections are shown as the mean fluorescent intensities (MFIs) of each microspot captured by ScanArray 5000A for the arrays stained with GNA (Fig. 1C) and 2G12 (Fig. 1D), respectively. Analysis of such microarray raw data in association with visual inspection of the microarray image (Fig. 1A), which contained

triplicate spots of a given antigen preparation, provided an evaluation of reproducibility and variation of this antigen microarray technology.

In Figures 2B, 3A and B, antigen-specific IgG or IgM reactivities are shown as microarray scores, which are the log2 transformed microarray values (mean-background). Each data point in these figures represents the mean of corresponding group, i.e., EAE *versus* normal controls (Fig. 2B), or MS *versus* OND (Fig. 3). The RAR scores specified in Figures 3C and D, and 4 were defined as the log2 transformed and IQR standardized microarray values. The IQR function in JMP-Genomics normalizes array data sets by setting their interquartile ranges (IQR) to be identical, which provides internally standardized data sets for further statistical evaluation of potential biomarkers.

An antigen-by-antigen analysis of variance (ANOVA) model was applied to obtain statistically significant differences between groups in comparison. Results are graphically presented as a volcano plot [Zink et al., 2013] for a global comparison of all RAR scores between the groups in comparison (Fig. 4A) and as One-way analysis scatterplots for selected targets (Fig. 4B and C). In the volcano plot, each dot represents a statistically weighted and quantified difference between MS and OND groups. The *x*-axis is the normalized difference (log2 scale) and the *y*-axis is −log10 (*P*-value) for the difference. Spots above the red dashed line represent signatures that differ significantly between the groups. For ANOVA scatterplots in Figures 2C, and 4B and C, each data point represents the mean of triplicate determinations. A Nominal Logistic Fit model was applied to assess the performance of a serum marker, e.g., M9_2G12_IgG (Fig. 4B, upper panel), as a classifier for differential diagnosis between MS and OND.

## Enzyme-Linked Immunosorbent Assay (ELISA) and Immunohistochemistry

ELISA assays were performed as described [Wang et al., 2002, 2013]. In brief, ELISA microtiter plates (NUNC, MaxiSorp, Thermo Scientific, Rochester, NY) coated with corresponding antigens, either Man9-BSA or $PLP_{139–151}$ at 10 μg/ml, were incubated with pre-titrated mouse serum (1:500). The captured antigen-specific IgG antibodies were revealed with a tagged Goat anti-mouse IgG second antibody. For lectin immunohistochemistry, biotinylated lectin preparations were applied to stain tissue sections. The tissue-bound lectins were developed with Streptavidin-HRP conjugate and DAB substrate. Lectins were pre-titrated and applied at 10 μg/ml in this study. A nonparametric statistical test (Wilcoxon rank-sum method) was used to calculate the significance of differences among comparative groups (Fig. 5).

## EAE Induction and Man9-KLH Coimmunization

For induction of EAE, we immunized 8–10-week-old female SJL mice (Jackson Laboratories, Bar Harbor, ME) with 100 μg sc of $PLP_{139–151}$ emulsified in complete Freund's adjuvant (CFA) at Day 0 without additional immunization. For the Man9-KLH co-immunization group, we applied the same immunization protocol as the EAE control group except with the inclusion of 100 μg of Man9-KLH in the immunization emulsion together with $PLP_{139–151}$ in CFA. We monitored clinical disease phenomena in the mice daily using the following scoring system: 0, no disease; 1, limp tail; 2, hindlimb weakness; 3, hindlimb

paralysis; 4, hindlimb and forelimb paralysis; 5, death. Mouse sera were taken at Day 0 before immunization and weekly after immunization for monitoring autoantibodies. Animal experiments were approved by and performed in compliance with the guidelines of the Stanford University Institutional Animal Care and Use Committee.

### Patient CSF Samples

All human samples were collected and used under protocols approved by the Institutional Review Boards of the Karolinska Institute and Stanford University. Patient demographics and clinical characteristics, including 10 RRMS, 1 SPMS, and 9 OND individuals are listed in Table 2. The levels of total IgG and IgM in these CSF specimens were measured by ELISA when this microarray study was performed. The mean values of total IgG in the MS group was 41.64 ± 28.41 μg/ml, which is significantly higher than those in the OND group (10.47 ± 6.34 μg/ml) ("t" test, $P = 0.005$). The levels of total IgM in the MS group (0.83 ± 0.04 μg/ml) were not different from those in the OND group (0.80 ± 0.07 μg/ml) ("t" test, $P = 0.218$).

## RESULTS

### Monitoring Autoantibodies that Target Self-Antigens of Distinct Molecular Structures

In this experiment, a panel of 51 antigens of diverse molecular structures was spotted in the same bioarray substrate (Table 1). These were protein and peptides of myelin sheath ($47^{\#}$–$51^{\#}$, $n = 5$), lipids/liposomes ($21^{\#}$–$46^{\#}$, $n = 26$), and carbohydrate antigens ($1^{\#}$–$20^{\#}$, $n = 20$). A panel of glycoconjugates that displayed cryptic glyco-epitopes, including high-mannose-clusters, M9_2G12-cluster ($3^{\#}$) and Man9-cluster ($4^{\#}$), was included in this array. Using these arrays, we analyzed serum samples from SJL/J mice immunized with myelin proteolipid protein peptide ($PLP_{139–151}$) [Kanteret al., 2006] for autoantibodies using a group of age-matched SJL/J mice as control.

Figure 2A shows representative microarray images in which the captured antigen-specific IgG (*Upper*) and IgM (*Bottom*) are shown for a mouse with EAE (*Right* column) and an age-matched control SJL/J mouse (*Left* column). Visual inspection of these microarray images identified four protein/peptide probes, PLP, myelin oligodendrocyte glycoprotein (MOG) and two preparations of myelin basic protein (MBP) (marked in red), that detected markedly increased autoantibodies of both IgG and IgM isotypes; two lipid probes, sulfatide and dimyristoylphosphatidylserine (DMPS, yellow), and two Man9-clusters (white), captured significant amounts of IgM, but not IgG, in the sample from this panel of mice with EAE.

A quantitative comparison of the two groups was conducted to examine the significance of these observations. Figure 2B shows the overlay plots of antibody profiles for the two groups where the levels of IgG and IgM antibodies are shown as the mean Ig scores of each group. Antibody values of the EAE group ($n = 10$) were colored in red and the controls ($n = 6$) in blue. The overall antibody profiles between the two groups appear similar with the exception of specific probes for autoantibodies to myelin proteins (MBPs [$48^{\#}$ and $49^{\#}$],

MOG [50#] and PLP [51#]), lipids (sulfatide [44#] and DMPS [46#]), and carbohydrate markers (M9_2G12-clusters [3#] and Man9-cluster [4#]).

Figure 2C illustrates results of the one-way ANOVA of four markers, including PTC (22), sulfatide (44), M9_2G12-cluster (3#), and Man9-cluster (4#). Similar to brain sulfatide (44), the two Man9-clusters (3# and 4#) captured increased amounts of autoantibodies of IgM isotype in EAE group as compared with the control group (NM). However, there was no difference between the two groups in induction of IgG autoantibodies for these markers.

These results demonstrate that the PLP-priming induced autoantibodies of both IgG and IgM isotypes to myelin proteins PLP, MOG, and MBP, but selectively elicited IgM responses to a number of lipid and carbohydrate antigens. The latter include autoantibodies to brain sulfatide and DMPS previously recognized using PVDF-immobilized lipid arrays [Kanter et al., 2006; Ho et al., 2012] and to carbohydrate-based novel markers, M9_2G12-clusters (3#) or Man9-cluster (4#).

## Autoantibodies Targeting High-Mannose-Clusters are Selectively Enriched in the CSF of MS Patients

We next examined whether the carbohydrate and lipid that detected antibodies in the EAE model might also detect autoantibodies in the CSF of MS patients and OND control subjects. For this purpose, we created a microarray displaying a panel of 32 carbohydrate and lipid probes for a focused investigation of nonprotein markers. The carbohydrate antigens that display N-glycan cryptic glyco-epitopes, e.g., AGOR (5#), ASOR (6#), and mannose clusters (1#, 3#, and 4#) [Wang, 2004, 2012b; Newsom-Davis et al., 2009; Wang et al., 2013] were included for microarray spotting (Figs. 3 and 4).

Figure 3A and B show the overlay plots of antibody profiles of the two groups. The colored needles that link the pairs of group means provide a global comparison of the antibody profiles between the MS group (*red circles*) and the OND group (*blue crosses*). This comparison reveals global differences in antibody profiles between the two groups. Specifically, the microarray scores of CSF-antibody activities in the MS group are generally higher than those seen in the CSF of OND subjects. These include not only anti-lipid antibodies (*Right, 26#–44#*), as previously reported [Ho et al., 2012], but also anti-carbohydrate antibodies (*Left, 1#–22#*). This observation may reflect the fact that the total Ig concentrations in the CSF of MS patients are higher than those in the CSF of OND subjects, which is one of the hallmarks of MS [Kabat et al., 1948, 1951; Steinman, 1996; Genain et al., 1999; Raine et al., 1999; Hueber et al., 2002].

We further examine whether there is any selective enrichment of antigen-specific antibodies in the CSF of MS patients. We reasoned that identifying such antibodies might provide clues to pinpoint key autoimmunogenic targets of MS. For this purpose, we introduced an approach to establish RAR scores for microarray detections and then seek targets that capture the antibody signal with higher RAR scores in MS patients. Specifically, we normalized microarray data sets by setting their IQR to be identical using the JMP-Genomics software package. This statistical operation effectively “quenches” the variation seen between subjects that is due to variable antibody concentrations in the CSF. The two

groups illustrate similar Ig-RAR profiles for both IgG and IgM antibody activities (Fig. 3C and D). However, a number of probes show higher IgG-RAR scores in the MS group than in the OND controls. These include two Man9-clusters ($3^{\#}$ and $4^{\#}$), three glucose polysaccharides, dextran N279 ($8^{\#}$), B1299S ($9^{\#}$), and B1355S ($10^{\#}$), and a Bacto-agar (20°C, extracted) antigen ($13^{\#}$) (Fig. 3C).

We then conducted an ANOVA analysis to identify antibody signatures that differed between the MS and OND groups based on a critical Bonferroni test. Figure 4A shows the results in a volcano plot [Zink et al., 2013], wherein each point represents a statistically weighted and quantified difference between the MS and OND groups. The *x*-axis is normalized difference in log2 scale ($RAR^{OND} - RAR^{MS}$) and the *y*-axis is − log10 (*P*-value) for the difference. Of the 126 antibody signatures captured in this assay (Fig. 3C and D), only two were above the cutoff line (−log10 [*P*-value] = 2.5) as highly significant differentiators between MS and OND. These were M9_2G12_IgG and Man9_IgG. Results of one-way ANOVA of the two Man9 clusters are shown in Figure 4B. Logistic regression analysis suggests that these CSF autoantibody signatures are highly significant in the differential diagnosis between MS and OND producing the area under the ROC curve values of 0.92929 and 0.87879, respectively. All other antibody signatures were weighted below the cutoff line (Fig. 4A), including four signatures that were variably higher in the MS group than in the OND group. These were N279_IgG ($P = 0.0825$), B1299S_IgG ($P = 0.0886$), B1355S_IgG ($P = 0.1135$), and Bacto_Agar_IgG ($P = 0.021$).

## Mannose-Clusters are Aberrantly Expressed in the CNS in EAE and MS

Based on the Bonferroni test recognition of the two high-mannose clusters, we hypothesized that the mannosyl glycans may be aberrantly expressed in vivo in MS/EAE subjects with exposure of these “cryptic” sugar moieties to trigger specific autoantibody responses. Therefore, we examined MS- and EAE-affected CNS tissues to determine whether they abnormally expressed high-mannose cluster-related carbohydrates. We applied lectins of known specificities to monitor expression of various *N*-glycan complex carbohydrates in MS and normal control brain tissue samples and in spinal cords of EAE mice (Fig. 5). The following three lectins were applied: (i) GNA, specific for the mannose-clusters; (ii) *Phaseolus vulgaris-L* (PHA-L), specific for Tri-II and m-II clusters; and (iii) *Sambucus nigra* I agglutinin (SNA-I), recognizing α2–6 linked Neu5Ac residues. The results of this study were: A) GNA: In normal human cerebral cortex (Fig. 5, **A0**), only the cytoplasm of neurons (red arrows) was stained. In an inflammatory MS lesion (**A1**), GNA stained a number of cell types, including cells with the morphological appearance of macrophages and reactive astrocytes (small red arrow). A dystrophic axon was also strongly positive (upper right corner, thick red arrow). In an acute inflammatory EAE lesion (**A2**), GNA stained many dystrophic axons (e.g., thick red arrow) and macrophage debris (e.g., thin red arrow). There was no positive staining in the spinal cords of control mice (data not shown). B) PHA-L: In normal human cerebral cortex (**B0**), PHA-L staining was negative. In an active MS lesion (B1), there was diffuse weak PHA-L staining. In the EAE lesion (**B2**), PHA-L staining was negative. C) SNA: SNA demonstrated positive staining of capillary endothelial cells in normal human cerebral cortex (**C0**) (red arrows). In the active MS lesion (**C1**), SNA selectively stained cells that were morphologically consistent with reactive microglia, (e.g.,

thick red arrow), as well as endothelial cells (small red arrows) (**C1**). In the EAE lesion (**C2**), SNA stained macrophage debris and endothelial cells (red arrows). In normal mice, SNA staining was limited to endothelial cells (data not shown).

Taken together, we observed that: (i) expression of high-mannose glycans, as defined by GNA, is restricted to cortical neurons in normal human brain tissue but is highly and broadly distributed in multiple cell types in tissues representing MS and EAE lesions; (ii) Tri/m-II chains detected by PHA-L were not exposed to lectin staining in normal brain tissue and were minimally expressed in active MS lesions; and (iii) α2-6Neu5Ac epitopes (SNA) that were present in blood vessels and red blood cells in normal brain tissue were aberrantly expressed in MS and EAE lesions. Thus, the repertoires of the aberrant carbohydrates in MS and EAE were not limited to the high-mannose N-glycan structures. This is indicated by the altered expression of the SNA epitopes (α2-6Neu5Ac) in these lesions.

### Induction of Anti-Oligomannose IgG Antibodies by Man9-KLH is Associated with the Reduced Clinical Severity of EAE

We next determined whether these carbohydrate targets could alter the course of EAE when used as immunogens co-delivered with myelin peptides emulsified in CFA. Kanter et al. took this approach to examine the in vivo effect of a lipid marker, sulfatide, which was identified as an MS and EAE-associated autoantigen by a lipid array analysis [Kanter et al., 2006]. They demonstrated that co-immunization of mice with sulfatide plus myelin peptide resulted in a more severe disease course and that the administration of anti-sulfatide antibody exacerbated EAE. In the present study, we co-immunized SJL mice with Man9-KLH together with myelin peptide $PLP_{139–151.}$ If the high-mannose-clusters were immunogenic, this immunization strategy should elicit antibodies targeting oligomannose antigens and if the anti-carbohydrate antibodies were pathogenic, induction of these antibodies should worsen the disease course. This in vivo validation experiment was conducted twice with similar outcomes. In the first test, 17 mice were used with 5 for the Man9-cluster experimental group and 12 for the PLP/CFA control group; the second test employed 20 mice with 10 for each group (Fig. 6).

As illustrated by the EAE score curves (Fig. 6A), active immunization by Man9-KLH plus PLP did not worsen but rather improved the course of EAE, although it elicited high-titers of anti-PLP IgG antibodies, as well as anti-oligomannose IgG antibodies (Fig. 6B). Although there was no difference in the titers of anti-PLP IgG antibodies between the PLP control and the Man9-co-immunization groups (Fig. 6C, right panel), the latter elicited markedly increased anti-Man9-IgG antibodies as determined by a glycan-specific ELISA assay (Fig. 6B, left panel).

## DISCUSSION

Applying integrated protein, lipid, and carbohydrate microarrays, we have characterized the autoantibody response in the PLP-induced EAE model in SJL/J mice. We found that the EAE-associated autoantibody profile was characterized by dominant IgG antibodies directed at myelin proteins with a broader spectrum of IgM antibodies targeting lipid- and carbohydrate-based autoantigens. IgM antibodies specific for brain sulfatide ($44^{\#}$) and

DMPS (46#) that were previously recognized by Kanter et al. [2006] were confirmed using this integrated multicomponent microarrays (Fig. 2). In addition, we detected anti-carbohydrate autoantibodies specific for the high-mannose type N-glycans (oligomannoses), M9_2G12-clusters (3#) and Man9-cluster (4#). Similar to anti-sulfatides, IgM but not IgG anti-oligomannose antibodies were detected in this panel of EAE mice (Fig. 2B).

Of note, the anti-oligomannose antibodies detected in EAE were also selectively enriched in the CSF of MS patients (Fig. 3). The specificities of the anti-mannose cluster autoantibodies detected in EAE were strikingly similar to those in the CSF of MS patients. Specifically, both EAE-derived and MS-d erived anti-oligomannose antibodies were similarly reactive with the two Man9-clusters, M9_2G12-clusters (3#) and Man9-cluster (4#). As illustrated in Figure 1B, the former is a Man9-tetramer conjugate and the latter a Man9-monomer conjugate. This binding profile is similar to lectin GNA (Fig. 1C) but differs from the binding profile of a human monoclonal antibody 2G12 (Fig. 1D) in our microarray assays. The antibody 2G12 is well characterized as an unusual, domain-exchanged IgG1 recognizing the Manα(1,2)Man moieties in dense cluster configurations of high-mannose type N-glycans as displayed on the outer domain of HIV gp120 glycoprotein [Calarese et al., 2003]. In our microarrays, 2G12 was highly reactive with the M9_2G12 cluster in [(Man9)4]n-cluster configuration, but only weakly reactive with Man9-cluster in the (Man9)n-configuration (Fig. 1D). In contrast, lectin GNA was strongly and equally reactive with the two oligomannose-conjugates (Fig. 1C). Thus, the binding specificities of the MS and EAE-associated anti-oligomannose autoantibodies overlap with the binding profile of GNA.

We examined whether the GNA-defined mannosyl glycan markers were expressed in the CNS. In normal brain tissues (Fig. 5 **A0**), GNA selectively stained the cytoplasmic compartment of human cortical neurons and was negative in other areas. In contrast, GNA was highly and broadly reactive with multiple cell types in MS lesions, including macrophages, reactive astrocytes and dystrophic axons (Fig. 5 **A1**). Similarly, this lectin stained many dystrophic axons and macrophage debris in the spinal cord lesions of mice with EAE (Fig. 5 **A2**). Thus, the GNA-defined mannosyl glycan markers were aberrantly expressed in inflammatory/demyelinating CNS lesions.

The EAE model provided a unique experimental condition to examine the potential immunogenicity of high-mannose-clusters in vivo. Specifically, we tested a Man9-KLH conjugate for its capacity to elicit an acquired immune response to oligomannose epitopes. We found that a single sc injection of the PLP/CFA emulsion containing Man9-KLH elicited highly significant anti-oligomannose IgG antibodies (Fig. 6B). Thus, this high-mannose-cluster-conjugate was immunogenic in vivo in this experimental condition. This effective anti-carbohydrate immunization may illuminate further development of novel vaccination strategy targeting the glycan markers of viruses [Calarese et al., 2003; Wang and Lu, 2004; Astronomo et al., 2008] and certain human cancers [Hakomori, 1985; Newsom-Davis et al., 2009; Wang, 2012b].

Moreover, we observed that induction of IgG anti-oligomannose response was associated with significantly reduced clinical signs of EAE (Fig. 6), a finding that is in contrast to the

results observed following administration of sulfatide in the same experimental setting in which a more severe disease course was observed [Kanter et al., 2006]. Further investigation will elucidate the physiological and/or pathological roles of anti-mannose cluster autoantibodies. Whether autoantibodies can play “Janus-like” opposing roles as CD47 does in autoimmune brain inflammation [Han et al., 2012] is under consideration. For example, the GNA-like autoantibodies that bind dystrophic axons and cell debris in MS/EAE lesions (Fig. 5) would be beneficial if they contributed to effective clearance of myelin debris that exposed the cryptic glyco-epitopes.

Exploring anti-glycan antibodies as potential serum biomarkers in differential diagnosis and prognosis of neurological disorders is an active research area [Willison, 2002; Willison and Yuki, 2002; Schwarz et al., 2003, 2006; Lolli et al., 2005; Brettschneider et al., 2009]. Notably, human serum IgM antibodies specific for a number of glucosyl targets have been investigated for MS diagnosis and prognosis [Schwarz et al., 2003, 2006; Brettschneider et al., 2009]. These include GAGA4 [Glc(α1,4)Glc(α)], GAGA6 [Glc(α1,6)Glc(α)], GAGA3 [Glc(α1,3)Glc(α)], and GAGA2 [Glc(α1,2)Glc (α)]. In the present study, we tested a panel of glucose polysaccharides, including dextran preparations of N279, B1299S, and B1355S [Wang and Kabat, 1996]. Dextran N279 predominantly displayed α(1,6)-internal chain epitopes, i.e., repetitive units of GAGA6 [Glc(α1, 6)Glc(α)]n as linear chains. B1299S was heavily branched and displays many terminal nonreducing end epitopes of [Glc(α1,6)Glc(α)]n. B1355S was characterized by α(1,3)α(1,6)linkages, which may present the GAGA3 [Glc(α1,3)Glc(α)]-moieties as both internal and terminal epitopes. However, this pilot study was limited in sample sizes, and it is difficult to conclude whether antibodies for these polysaccharides were significantly enriched in the CSF of MS subjects (Fig. 4C).

In addition to these glucose polysaccharides, we observed CSF-enrichment of anti-Bacto-agar IgG antibodies in the CSF of MS subjects. The Bacto-agar preparation (20°C, extracted) is a pyruvylated galatosyl polysaccharide with [4,6pyDGalβ1]-epitopes, which are also present in microbial polysaccharides, e.g., *Klebsiella* K30 and K33 [Kabat et al., 1980]. Anti-Dextran and anti-Bacto-agar antibodies are often present in the human circulation [Kabat and Berg, 1953; Wang et al., 2002]. Detection of these common anti-carbohydrate antibodies in both CSF and blood may have utility in monitoring the functional integrity of the blood-brain barrier. These findings must be further validated in a larger cohort of MS and OND subjects. Shared carbohydrate determinants on microbes and brain tissue, such as manosyl moieties, represents yet another pathway where the microbiome and autoimmunity intersect in neuroinflammatory disease states [Wang et al., 2002; Wang and Lu, 2004; Yuki et al., 2004; Shahrizaila and Yuki, 2011; Ogawa et al., 2013].

## Acknowledgments

We acknowledge Dr. Russell Wolfinger and the technical support team of SAS Institute for their instruction and excellent technical assistance in the use of JMP and JMP-Genomics software; Dr. Jennifer L. Kanter, Professors William H. Robinson, Leonore A. Herzenberg, and Leonard A. Herzenberg for helpful discussions, Dr. Jiahong Ni for preparation of [(Man9)4]n-KLH conjugate, Drs. Rachel Schneerson and John Robbins for Shigella dysenteriae Type 1 O-specific polysaccharide, and the late Professor Elvin A. Kabat and his previous students, postdoctoral fellows, and collaborators for their contributions to a number of carbohydrate antigens listed in Table 1 that were used in this study. This work is supported in part by NIH grants R01NS055997 (L. Steinman and D. Wang), U01CA128416 and R56AI108388 (D. Wang), and R01AI067111 (L-X. Wang), and by the Swedish Research Council and the Knut and Alice Wallenberg Foundation (TO).

## References


Astronomo RD, Lee HK, Scanlan CN, Pantophlet R, Huang CY, Wilson IA, Blixt O, Dwek RA, Wong CH, Burton DR. A glycoconjugate antigen based on the recognition motif of a broadly neutralizing human immunodeficiency virus antibody, 2G12, is immunogenic but elicits antibodies unable to bind to the self glycans of gp120. J Virol. 2008; 82:6359–6368. [PubMed: 18434393]

Beyer NH, Lueking A, Kowald A, Frederiksen JL, Heegaard NH. Investigation of autoantibody profiles for cerebrospinal fluid biomarker discovery in patients with relapsing-remitting multiple sclerosis. J Neuroimmunol. 2012; 242:26–32. [PubMed: 22177943]

Breloy I, Pacharra S, Aust C, Hanisch FG. A sensitive gel-based global O-glycomics approach reveals high levels of mannosyl glycans in the high mass region of the mouse brain proteome. Biol Chem. 2012a; 393:709–717. [PubMed: 22944674]

Breloy I, Pacharra S, Ottis P, Bonar D, Grahn A, Hanisch FG. O-linked N,N′-diacetyllactosamine (LacdiNAc)-modified glycans in extracellular matrix glycoproteins are specifically phosphorylated at subterminal N-acetylglucosamine. J Biol Chem. 2012b; 287:18275–18286. [PubMed: 22474328]

Brettschneider J, Jaskowski TD, Tumani H, Abdul S, Husebye D, Seraj H, Hill HR, Fire E, Spector L, Yarden J, et al. Serum anti-GAGA4 IgM antibodies differentiate relapsing remitting and secondary progressive multiple sclerosis from primary progressive multiple sclerosis and other neurological diseases. J Neuroimmunol. 2009; 217:95–101. [PubMed: 19879655]

Brooks, SA.; Dwek, MV.; Schumacher, U. Functional & Molecular Glycobiology. Oxford: BIOS Scientific Publishers Ltd; 2002.

Calarese DA, Scanlan CN, Zwick MB, Deechongkit S, Mimura Y, Kunert R, Zhu P, Wormald MR, Stanfield RL, Roux KH, et al. Antibody domain exchange is an immunological solution to carbohydrate cluster recognition. Science. 2003; 300:2065–2071. [PubMed: 12829775]

Chai W, Yuen CT, Feizi T, Lawson AM. Core-branching pattern and sequence analysis of mannitol-terminating oligosaccharides by neoglycolipid technology. Anal Biochem. 1999a; 270:314–322. [PubMed: 10334849]

Chai W, Yuen CT, Kogelberg H, Carruthers RA, Margolis RU, Feizi T, Lawson AM. High prevalence of 2-mono- and 2,6-di-substituted manol-terminating sequences among O-glycans released from brain glycopeptides by reductive alkaline hydrolysis. Eur J Biochem. 1999b; 263:879–888. [PubMed: 10469154]

Genain CP, Cannella B, Hauser SL, Raine CS. Identification of autoantibodies associated with myelin damage in multiple sclerosis. Nat Med. 1999; 5:170–175. [PubMed: 9930864]

Hakomori S. Aberrant glycosylation in cancer cell membranes as focused on glycolipids: overview and perspectives. Cancer Res. 1985; 45:2405–2414. [PubMed: 3886132]

Han MH, Lundgren DH, Jaiswal S, Chao M, Graham KL, Garris CS, Axtell RC, Ho PP, Lock CB, Woodard JI, et al. Janus-like opposing roles of CD47 in autoimmune brain inflammation in humans and mice. J Exp Med. 2012; 209:1325–1334. [PubMed: 22734047]

Ho PP, Kanter JL, Johnson AM, Srinagesh HK, Chang EJ, Purdy TM, van Haren K, Wikoff WR, Kind T, Khademi M, et al. Identification of naturally occurring fatty acids of the myelin sheath that resolve neuroinflammation. Sci Transl Med. 2012; 4:137ra73.

Hueber W, Utz PJ, Steinman L, Robinson WH. Autoantibody profiling for the study and treatment of autoimmune disease. Arthritis Res. 2002; 4:290–295. [PubMed: 12223102]

Kabat EA, Berg D. Dextran; an antigen in man. J Immunol. 1953; 70:514–532. [PubMed: 13069714]

Kabat EA, Glusman M, Knaub V. Immunochemical estimation of albumin and gamma globulin in normal and pathological cerebrospinal fluid. Trans Am Neurol Assoc. 1948; 73(73 Annual Meet): 93. [PubMed: 18111263]

Kabat EA, Wolf A, Bezer AE, Murray JP. Studies on acute disseminated encephalomyelitis produced experimentally in rhesus monkeys. J Exp Med. 1951; 93:615–633. [PubMed: 14832406]

Kabat EA, Liao J, Bretting H, Franklin EC, Geltner D, Frangione B, Koshland ME, Shyong J, Osserman EF. Human monoclonal macroglobulins with specificity for Klebsiella K polysaccharides that contain 3,4-pyruvylated-D-galactose and 4,6-pyruvylated-D-galactose. J Exp Med. 1980; 152:979–995. [PubMed: 6158553]

Kanter JL, Narayana S, Ho PP, Catz I, Warren KG, Sobel RA, Steinman L, Robinson WH. Lipid microarrays identify key mediators of autoimmune brain inflammation. Nat Med. 2006; 12:138–143. [PubMed: 16341241]

Lehmann PV, Forsthuber T, Miller A, Sercarz EE. Spreading of T-cell autoimmunity to cryptic determinants of an autoantigen. Nature. 1992; 358:155–157. [PubMed: 1377368]

Lolli F, Mulinacci B, Carotenuto A, Bonetti B, Sabatino G, Mazzanti B, D'Ursi AM, Novellino E, Pazzagli M, Lovato L, et al. An N-glucosylated peptide detecting disease-specific autoantibodies, biomarkers of multiple sclerosis. Proc Natl Acad Sci USA. 2005; 102:10273–10278. [PubMed: 16014416]

McRae BL, Vanderlugt CL, Dal Canto MC, Miller SD. Functional evidence for epitope spreading in the relapsing pathology of experimental autoimmune encephalomyelitis. J Exp Med. 1995; 182:75–85. [PubMed: 7540658]

Michele DE, Campbell KP. Dystrophin-glycoprotein complex: post-translational processing and dystroglycan function. J Biol Chem. 2003; 278:15457–15460. [PubMed: 12556455]

Newsom-Davis TE, Wang D, Steinman L, Chen PF, Wang LX, Simon AK, Screaton GR. Enhanced immune recognition of cryptic glycan markers in human tumors. Cancer Res. 2009; 69:2018–2025. [PubMed: 19223535]

Ogawa G, Kaida K, Kuwahara M, Kimura F, Kamakura K, Kusunoki S. An antibody to the GM1/GalNAc-GD1a complex correlates with development of pure motor Guillain-Barre syndrome with reversible conduction failure. J Neuroimmunol. 2013; 254:141–145. [PubMed: 23000056]

Pacharra S, Hanisch FG, Breloy I. Neurofascin 186 is O-mannosylated within and outside of the mucin domain. J Proteome Res. 2012; 11:3955–3964. [PubMed: 22746206]

Raine CS, Cannella B, Hauser SL, Genain CP. Demyelination in primate autoimmune encephalomyelitis and acute multiple sclerosis lesions: a case for antigen-specific antibody mediation. Ann Neurol. 1999; 46:144–160. [PubMed: 10443879]

Robinson WH, DiGennaro C, Hueber W, Haab BB, Kamachi M, Dean EJ, Fournel S, Fong D, Genovese MC, de Vegvar HE, et al. Autoantigen microarrays for multiplex characterization of autoantibody responses. Nat Med. 2002; 8:295–301. [PubMed: 11875502]

Robinson WH, Fontoura P, Lee BJ, de Vegvar HE, Tom J, Pedotti R, DiGennaro CD, Mitchell DJ, Fong D, Ho PP, et al. Protein microarrays guide tolerizing DNA vaccine treatment of autoimmune encephalomyelitis. Nat Biotechnol. 2003; 21:1033–1039. [PubMed: 12910246]

Schachter H. The "yellow brick road" to branched complex N-glycans. Glycobiology. 1991; 1:453–461. [PubMed: 1840403]

Schwarz M, Spector L, Gargir A, Shtevi A, Gortler M, Altstock RT, Dukler AA, Dotan N. A new kind of carbohydrate array, its use for profiling antiglycan antibodies, and the discovery of a novel human cellulose-binding antibody. Glycobiology. 2003; 13:749–754. [PubMed: 12851287]

Schwarz M, Spector L, Gortler M, Weisshaus O, Glass-Marmor L, Karni A, Dotan N, Miller A. Serum anti-Glc(alpha1, 4)Glc(alpha) antibodies as a biomarker for relapsing-remitting multiple sclerosis. J Neurol Sci. 2006; 244:59–68. [PubMed: 16480743]

Shahrizaila N, Yuki N. Antiganglioside antibodies in Guillain-Barre syndrome and its related conditions. Expert Rev Neurother. 2011; 11:1305–1313. [PubMed: 21864076]

Steinman L. Multiple sclerosis: a coordinated immunological attack against myelin in the central nervous system. Cell. 1996; 85:299–302. [PubMed: 8616884]

Trkola A, Purtscher M, Muster T, Ballaun C, Buchacher A, Sullivan N, Srinivasan K, Sodroski J, Moore JP, Katinger H. Human monoclonal antibody 2G12 defines a distinctive neutralization epitope on the gp120 glycoprotein of human immunodeficiency virus type 1. J Virol. 1996; 70:1100–1108. [PubMed: 8551569]

Walker LM, Huber M, Doores KJ, Falkowska E, Pejchal R, Julien JP, Wang SK, Ramos A, Chan-Hui PY, Moyle M, et al. Broad neutralization coverage of HIV by multiple highly potent antibodies. Nature. 2011; 477:466–470. [PubMed: 21849977]

Wang D. Carbohydrate microarrays. Proteomics. 2003; 3:2167–2175. [PubMed: 14595816]

Wang, D. Carbohydrate antigens. In: Meyers, RA., editor. Encyclopedia of Molecular Cell Biology and Molecular Medicine. Wiley-VCH; Weinheim, Germany: 2004. p. 277-301.p. II

Wang D. Carbohydrate antigen microarrays. Methods Mol Biol. 2012a; 808:241–249. [PubMed: 22057530]

Wang D. N-glycan cryptic antigens as active immunological targets in prostate cancer patients. J Proteomics Bioinform. 2012b; 5:90–95.

Wang, D.; Kabat, EA. Carbohydrate antigens (polysaccharides). In: Regenmortal, MHVV., editor. Structure of Antigens. Boca Raton, New York, London, Tokyo: CRC Press; 1996. p. 247-276.

Wang D, Lu J. Glycan arrays lead to the discovery of autoimmunogenic activity of SARS-CoV. Physiol Genomics. 2004; 18:245–248. [PubMed: 15161967]

Wang D, Liu S, Trummer BJ, Deng C, Wang A. Carbohydrate microarrays for the recognition of cross-reactive molecular markers of microbes and host cells. Nat Biotechnol. 2002; 20:275–281. [PubMed: 11875429]

Wang D, Herzenberg LA, Steinman L. A lipid-based microarray and methods of use thereof. PCT International application No PCT/US2006/011544, filed March 22 2006. 2005 claiming benefit of U.S. Provisional Application no. 60/664 251 filed March 20, 2005.

Wang D, Dafik L, Nolley R, Huang W, Wolfinger RD, Wang LX, Peehl DM. Anti-oligomannose antibodies as potential serum biomarkers of aggressive prostate cancer. Drug Dev Res. 2013; 74:65–80. Biomarkers in Drug Development and Companion Diagnostics.

Willison HJ. Anti-glycolipid antibodies in the diagnosis of autoimmune neuropathies. Rev Neurol (Paris). 2002; 158 (12 Pt 2):S16–S20. [PubMed: 12690656]

Willison HJ, Yuki N. Peripheral neuropathies and anti-glycolipid antibodies. Brain. 2002; 125 (Pt 12): 2591–2625. [PubMed: 12429589]

Yu M, Johnson JM, Tuohy VK. Generation of autonomously pathogenic neo-autoreactive Th1 cells during the development of the determinant spreading cascade in murine autoimmune encephalomyelitis. J Neurosci Res. 1996a; 45:463–470. [PubMed: 8872907]

Yu M, Johnson JM, Tuohy VK. A predictable sequential determinant spreading cascade invariably accompanies progression of experimental autoimmune encephalomyelitis: a basis for peptide-specific therapy after onset of clinical disease. J Exp Med. 1996b; 183:1777–1788. [PubMed: 8666934]

Yuen CT, Chai W, Loveless RW, Lawson AM, Margolis RU, Feizi T. Brain contains HNK-1 immunoreactive O-glycans of the sulfoglucuronyl lactosamine series that terminate in 2-linked or 2,6-linked hexose (mannose). J Biol Chem. 1997; 272:8924–8931. [PubMed: 9083013]

Yuki N, Susuki K, Koga M, Nishimoto Y, Odaka M, Hirata K, Taguchi K, Miyatake T, Furukawa K, Kobata T, et al. Carbohydrate mimicry between human ganglioside GM1 and Campylobacter jejuni lipooligosaccharide causes Guillain-Barre syndrome. Proc Natl Acad Sci USA. 2004; 101:11404–11409. [PubMed: 15277677]

Zink RC, Wolfinger RD, Mann G. Summarizing the incidence of adverse events using volcano plots and time intervals. Clin Trials. 2013; 10:398–406. [PubMed: 23690094]

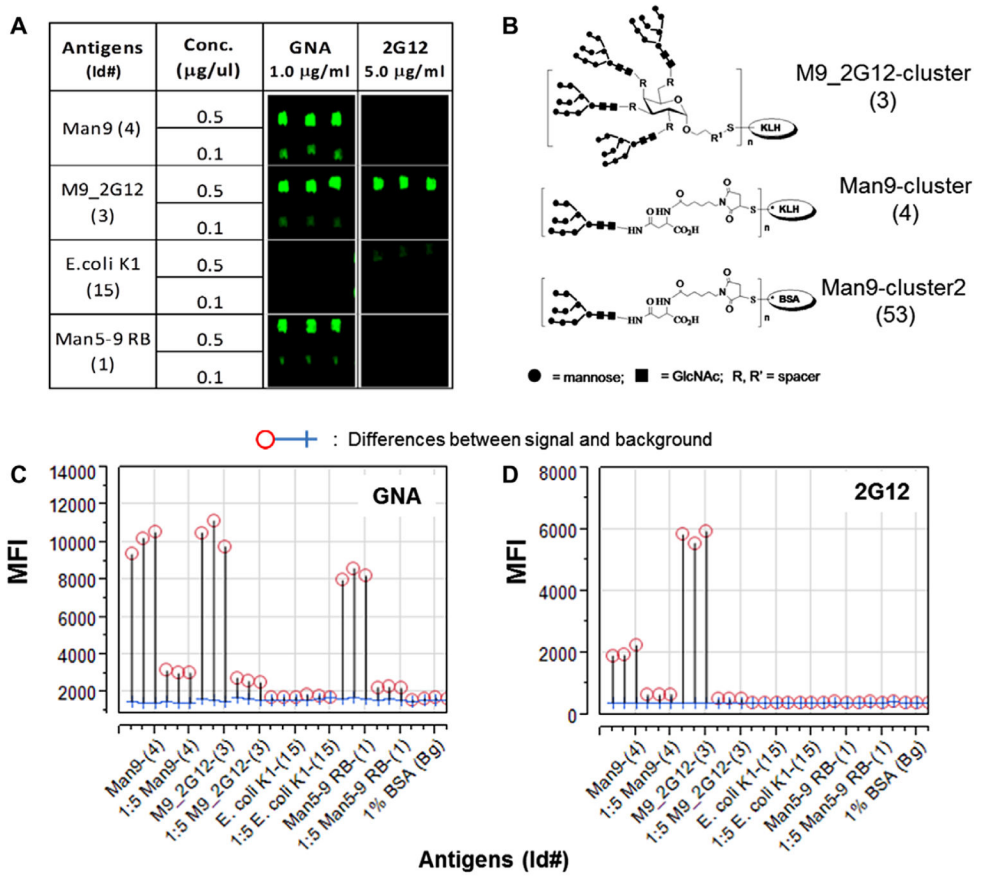


**Fig. 1.**

A carbohydrate microarray analysis of oligomannosyl antigens for expression of the 2G12-like and GNA-like glyco-epitopes. The mannose-cluster-containing microarrays were stained with 2G12 (5 µg/ml) and a biotinylated GNA (1.0 µg/ml), respectively. The former was revealed by Alexa$^{647}$-tagged Goat anti-human IgG-Fc-specific antibodies at 2 µg/ml; then developed with Streptavidin-Cy5 conjugate at 2 µg/ml. (**A**) Microarray images stained with either GNA or 2G12. (**B**) Cluster configuration of the three Man9-conjugates. Microarray detections are shown as the mean fluorescent intensities (MFIs) of each microspot as captured by the ScanArray 5000A for the arrays stained with GNA (**C**) and 2G12 (**D**), respectively. Results were compared using overlay plots of the MFIs of staining signal (*circles*) versus those of local backgrounds surrounding the antigen microarrays (*crosses*) (**C** and **D**). [Color figure can be viewed in the online issue which is available at wileyonlinelibrary.com]

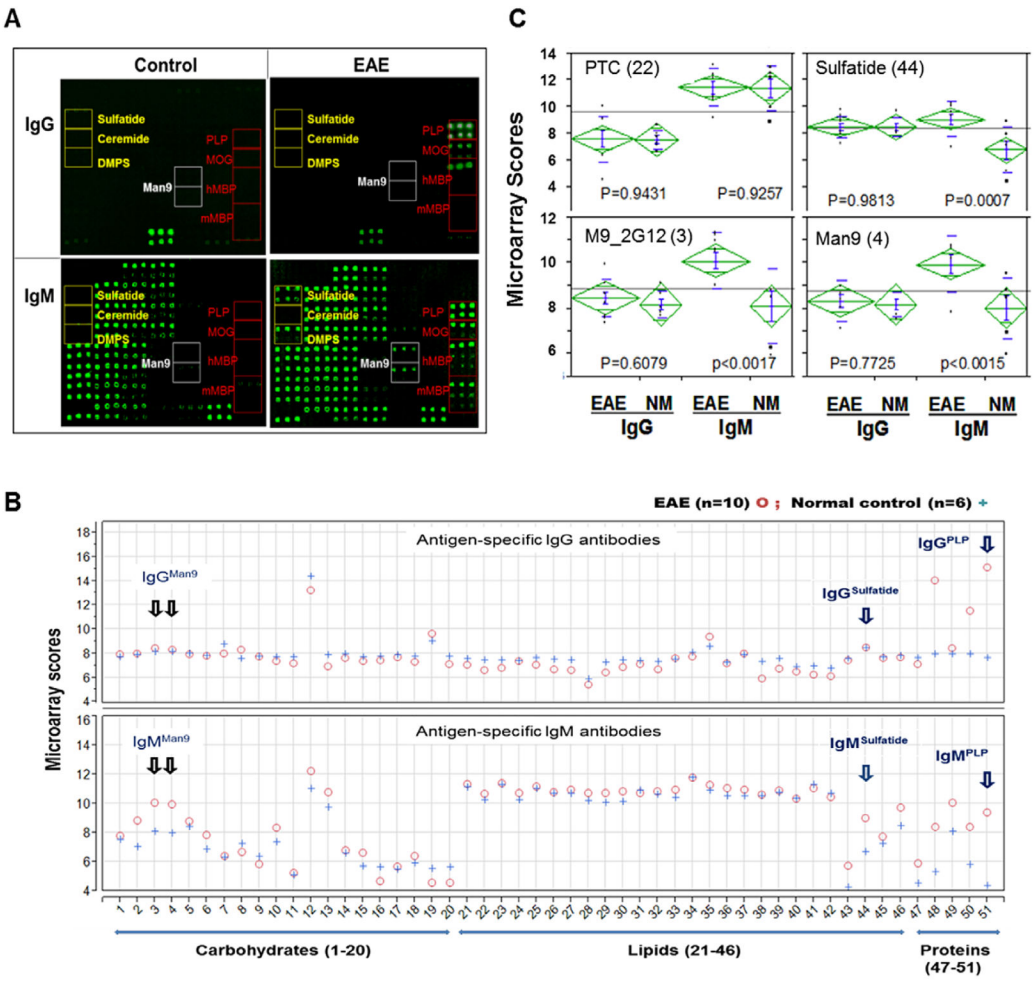


**Fig. 2.**

Epitope spreading to a broad range of protein, peptides, lipids, and carbohydrates in the serum of mice with EAE detected by integrated microarrays. A panel of 51 antigenic structures (Table 1) was spotted in a versatile bioarray substrate in triplicate in 2–4 dilutions to generate a total of 312 microspots of antigens per array. This platform supports detection of 208 unique antibody signatures, including 104 IgG- and 104 IgM-antibody signatures. (**A**) Each array was stained with a serum sample at a 1:25 dilution from a mouse with *EAE* (*Right*) or age-matched control SJ/L mouse (*Left*). The captured IgG (*Upper* array images) were stained with an anti-IgG antibody conjugated with Cy5 at 2 μg/ml and the captured IgM in the same array (*Bottom*) was revealed by an R-PE-tagged anti-IgM secondary antibody at 2 μg/ml. Array locations of myelin proteins (PLP, MOG and MBP), lipids/liposomes (sulfatide, ceramide and DMPS), and high-mannose-clusters (Man9) are boxed. (**B**), the levels of IgG and IgM antibodies are shown as mean Ig scores of each group and presented in separate overlay plots. Ig values of the *EAE* group ($n = 10$) are marked as circles and the controls ($n = 6$) as crosses. *Microarray scores: Antigen-specific IgG or IgM reactivities are shown as microarray scores, the log2 transformed (mean-background) values of microarray detection. (**C**) Results of the statistical analysis of the four probes, including two lipid antigens, PTC and sulfatide and two mannose-clusters, M9_2G12 and Man9. EAE

mice examined in this experiment were induced by immunizing SJL/J mice with myelin $PLP_{139–151}$ as described [Kanter et al., 2006]. [Color figure can be viewed in the online issue which is available at wileyonlinelibrary.com]

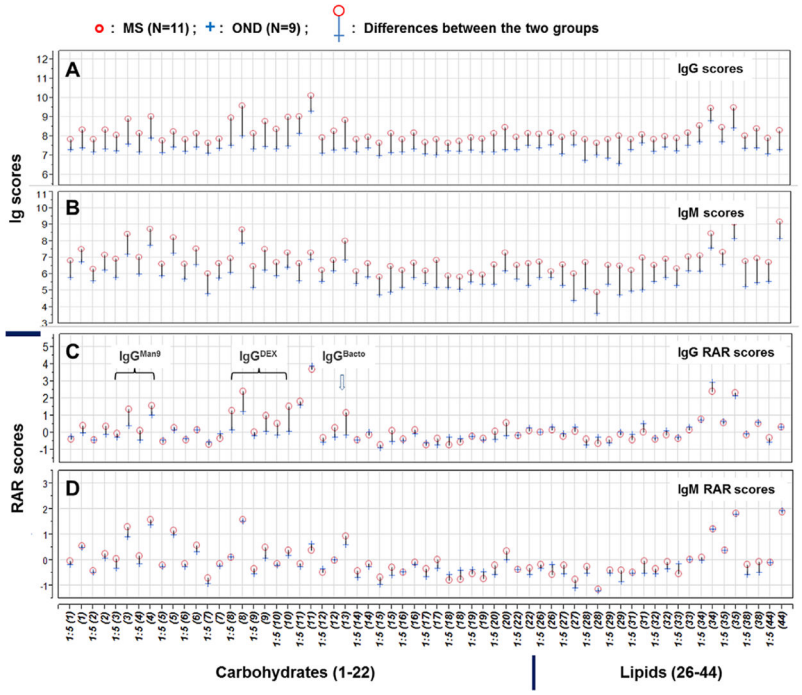


**Fig. 3.**

Integrated lipid/carbohydrate arrays recognize globally elevated antigen-specific antibodies in the CSF of MS patients as compared with those detected in the OND CSF. CSF samples from 11 MS (10 RRMS and 1 SPMS) and 9 OND subjects were characterized using microarrays spotted with 12 lipid and 20 carbohydrate antigens. Each preparation was spotted in triplicate at 2–4 dilutions. As illustrated in the overlay plots (**A–D**), this microarray supports detection of 126 unique antibody signatures. These included 63 IgG (**A** and **C**) and 63 IgM (**B** and **D**) signatures. Anti-human IgG or IgM secondary antibodies were used to reveal the antigen-specific antibodies detected by these microarrays. The captured IgG were stained with an anti-human IgG antibody conjugated with Cy3 at 2 μg/ml and the captured IgM in the same array revealed by a biotinylated anti-human IgM secondary antibody at 2 μg/ml and developed with Streptavidin-Cy5 conjugate at 2 μg/ml. Microarray data sets in **A** and **B** were processed as described in legend to Figure 1 and illustrated as microarray scores. In **C** and **D**, microarray data sets were further processed using JMP-Genomics to produce *RAR scores. The results are presented as overlay plots of the mean microarray scores for each group. The colored needles that link the group means of each pair of the scores provide a global comparison of antibody profiles of MS group (*circles*) and OND (*crosses*). **RAR Score: RAR*—Relative Antibody Reactivity, the value of log2 transformed and IQR-standardized microarray value (Mean-background). For each antigen in a given concentration, the mean value of triplicate array detections was calculated.

[Color figure can be viewed in the online issue which is available at wileyonlinelibrary.com]

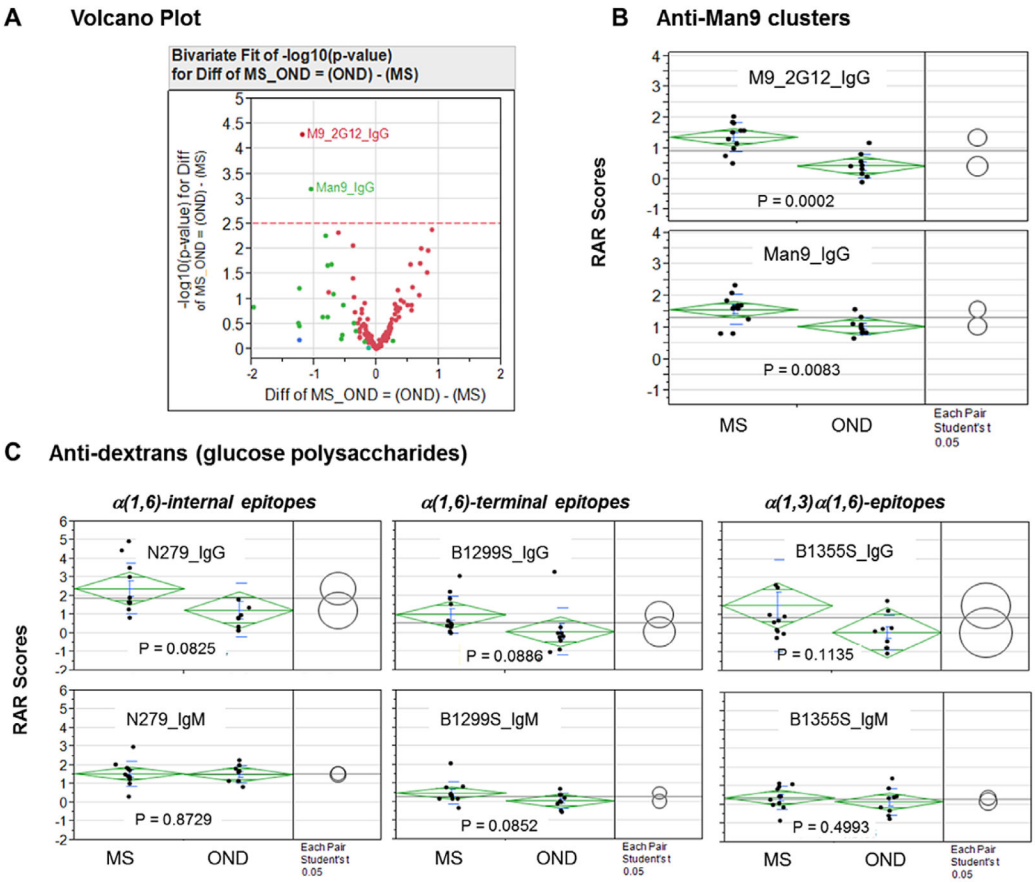


**Fig. 4.**

MS-associated autoantibodies in CSF samples target high-mannose clusters, the cores of N-glycans. (**A**) Volcano plot analysis of the RAR scores of all antibody signatures. In the volcano plot, each point represents a biologically unique feature captured by the microarray, i.e., a normalized difference for a specific antibody signature ($RAR^{MS}$-$RAR^{OND}$). The *x*-axis is the normalized difference (log2 scale); the *y*-axis is −log10 (*P*-value), which weights the levels of significance of a difference. Points above the dashed line (cutoff level 2.5) represent signatures that differ significantly between the groups based on the Bonferroni test. Two signatures, M9_2G12_IgG and Man9_IgG, were identified by this critical statistical test as highly significant markers. In **B** and **C**, One-way analysis was performed to compare group means among the selected carbohydrate antigens listed in each panel. Each point in the panels represents the mean value (RAR score) of triplicate array detection of a subject. The means are shown as bars and standard deviations as diamonds around the mean value. The comparison circles for Student's "t"-test appear to the right of the mean diamonds to illustrate the significance of the differences among the means. By graphically showing the intersections, these circles allow visual inspection of the significance of differences. The more the circles intersect, the less significant their difference, and vice versa. [Color figure can be viewed in the online issue which is available at wileyonlinelibrary.com]

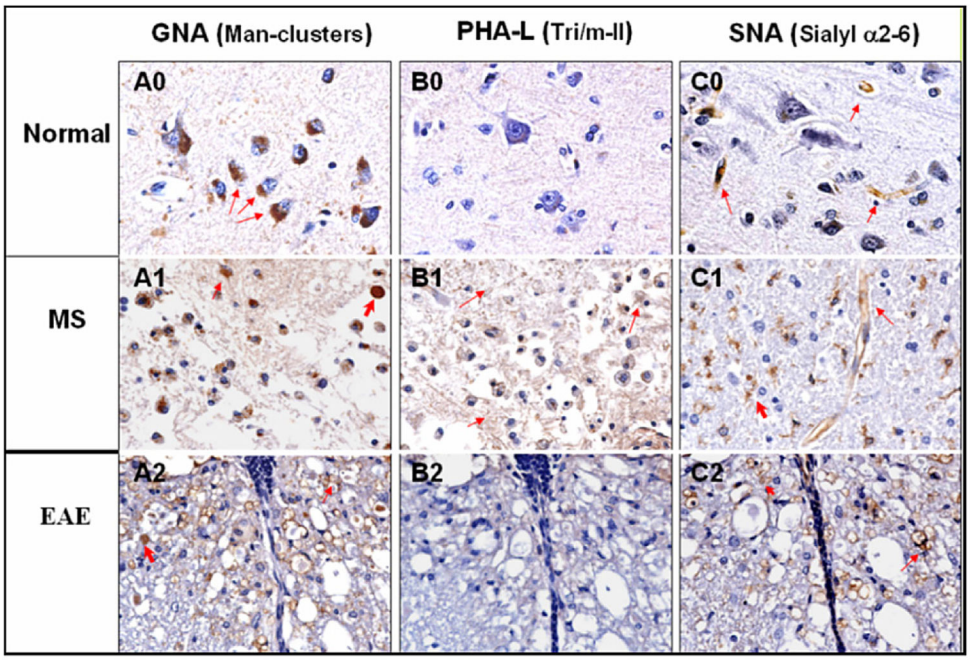


**Fig. 5.**

Lectin GNA, PHA-L and SNA histochemistry of human brain tissues, normal (0) and MS (1), and mouse spinal cord EAE lesions (2). CNS tissues were stained with biotinylated lectins and developed with Streptavidin-HRP conjugate and DAB substrate. Lectins were pre-titrated and applied at 10 μg/ml for tissue staining. Column A, B, and C were stained with lectin GNA, PHA-L and SNA respectively. Normal: A0, B0, and C0; MS: A1, B1, and C1; EAE: A2, B2, and C2. The carbohydrates recognized by the lectins are indicated for each column.

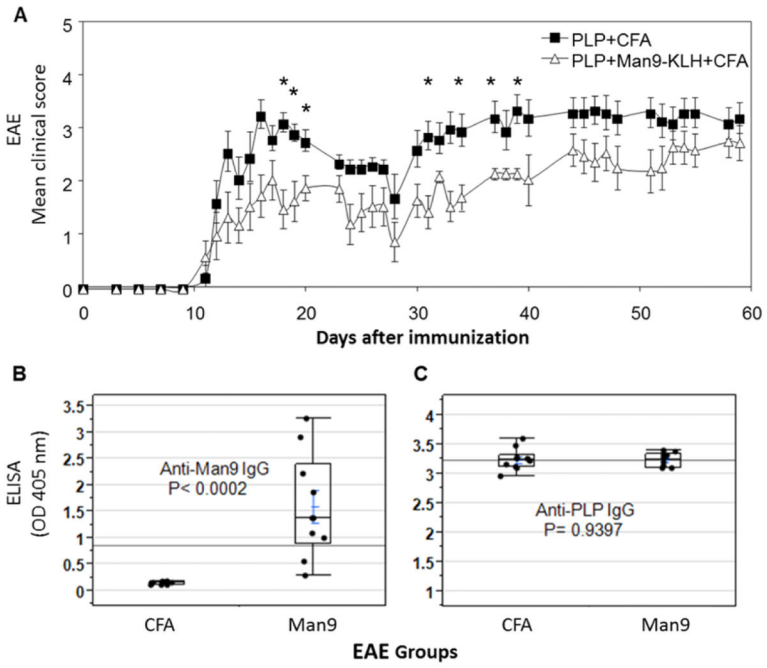


**Fig. 6.**

Induction of anti-Man9-Cluster IgG antibodies by co-immunization with mannose-clusters and a pathogenic myelin peptide does not worsen the course of EAE. (**A**) Overlay plot of the EAE scores of Man9 group (-△-, *n* = 10) and those of vehicle control group (-■-, *n* = 10). *Man9 group*: Co-immunization of SJL mice with Man9-KLH (100μg/mouse) and $PLP_{139–151}$ (100μg/mouse) emulsified in CFA. *Vehicle control group:* immunization with PLP plus CFA without additional immunogen. Each point represents the mean ± s.e.m. A statistical test (Mann–Whitney test) was used to calculate the significance of differences between the two groups. The time points illustrated significant differences ($P < 0.05$) are marked * on the graph. (**B**) Anti-Man9 IgG and (**C**) anti-PLP IgG responses analysed by ELISA. Serum specimens from the EAE experiment (Fig. 6A) were titrated for antigen-specific ELISA in a preliminary experiment and applied at 1:500 dilutions for ELISA detection of antigen-specific IgG. (**B**) ELISA plates coated with Man9-BSA conjugate at 10 μg/ml for detection of Man9-specific IgG at day 21 post-immunization with Man9-KLH and PLP; (**C**) ELISA plates were coated with $PLP_{139–151}$ at 10 μg/ml for the detection of PLP-specific IgG in the same serum specimen. Serum antibodies specific for the carrier BSA in day 0 pre-immunization and day 21 post-immunization and pre-existing anti-Man9 and anti-PLP in day 0 sera were below the detection sensitivity of this ELISA (OD 405 nm = or <0.150). One-way ANOVA was performed to compare the ELISA results obtained between groups. A nonparametric statistical test (Wilcoxon rank-sum method) was applied to calculate the significance of differences between comparative groups.

**TABLE 1**

Antigen Preparations Used in This Study

| Antigen ID# | Antigen name | Antgen preparations* | Description | Source | References |
|---|---|---|---|---|---|
| 1 | Man5_9-RB | Man 5–9 RB, 0.5 mg/ml | Ribonuclease B with $Man_{5–6}$ $GlcNAc_2$ Asn as the main glycans (pancreas, bovine) | Sigma-Aldrich | This report |
| 2 | KLH-SH | KLH-SH, 0.5 mg/ml | Thiolated keyhole limpet hemocyanin | Present authors | Ni et al., Bioconjug Chem., 17:493–500 (2006) |
| 3 | M9(2G12) | Man9-Cluster(2G12)-KLH, 0.5 mg/ml | $[(Man9GlcNAc2Asn)_4]_n$-KLH | Present authors | Ni et al., Bioconjug Chem., 17:493–500 (2006) |
| 4 | Man9 Man9-KLH | $(Man9GlcNAc2Asn)_n$-KLH, 0.5 mg/ml | Present authors | Ni et al., Bioconjug Chem., 17:493–500 (2006) | |
| 5 | AGOR | AGOR, 0.5 mg/ml | Agalacto-orosomucoid | From the late Prof. Elvin A. Kabat (Columbia University) | Wang & Lu, Physiol Genomics 18(2):245–8, (2004) |
| 6 | ASOR | ASOR, 0.5 mg/ml | Asialo-orosomucoid | From the late Prof. Elvin A. Kabat (Columbia University) | Wang & Lu, Physiol Genomics 18(2):245–8, (2004) |
| 7 | OR | OR, 0.5 mg/ml | Orosomucoid (human α1-acid glycoprotein) | Sigma-Aldrich | Wang & Lu, Physiol Genomics 18(2):245–8, (2004) |
| 8 | N279 | N279, 0.5 mg/ml | α(1→6)dextran, NRRL N279 | Northern Regional research laboratory, (Peoria, IL) NRRL B-2448 | Wang, et al., Nat Biotechnol 20(3):275–81, (2002) |
| 9 | B1299S | B1299S, 0.5 mg/ml | α(1→6)dextran, NRRL B-1299S | Northern Regional research laboratory, (Peoria, IL) NRRL B-2448 | Wang, et al., Nat Biotechnol 20(3):275–81, (2002) |
| 10 | B1355S | B1355S, 0.5 mg/ml | α(1→3)(1→6)dextran, NRRL B-1355S | Northern Regional research | Wang, et al., Nat |

| Antigen ID# | Antigen name | Antgen preparations* | Description | Source | References |
|---|---|---|---|---|---|
| | | | | laboratory, (Peoria, IL) NRRL B-2448 | Kabat et al., J. Exp. Med. 164, 642 (1986) |
| 11 | B2448 | B2448, 0.5 mg/ml | Phosphomannan, NRRL B-2448 | Northern Regional research laboratory, (Peoria, IL) NRRL B-2448 | Kabat et al., J. Exp. Med. 164, 642 (1986) |
| 12 | Levan | Levan, 0.5 mg/ml | Levan (from preparation of B-512-E dextran) | Commercial Solvents Co. (Terre Haute, IN) | Kabat et al., J. Exp. Med. 164, 642 (1986) |
| 13 | Bacto-Agar | Bacto-Agar, 0.5 mg/ml | Bacto-agar 20°C extract | From the late Prof. Elvin A. Kabat (Columbia University) | Duckworth & Yaphe, Carbohydr. Res. 16, 189 (1971) |
| 14 | E. coli. 2630 | E. coli. LPS 2630, 0.5 mg/ml | Lipopolysaccharides from Escherichia coli 0111:B4 | Sigma-Aldrich | This report |
| 15 | E. coli. K1 | E. coli. K1 CP, 0.5 mg/ml | E. coli K1 capsular polysaccharide (CP) | From the late Prof. Elvin A. Kabat (Columbia University) | Kabat et al., J. Exp. Med. 164, 642 (1986) |
| 16 | E. coli. K100 | E. coli. K100 CP, 0.5 mg/ml | E. coli K100 capsular polysaccharide (CP) | From the late Prof. Elvin A. Kabat (Columbia University) | Kabat et al., J. Exp. Med. 164, 642 (1986) |
| 17 | E. coli. K92 | E. coli. K92 CP, 0.5 mg/ml | E. coli K92 capsular polysaccharide | From the late Prof. Elvin A. Kabat (Columbia University) | Kabat et al., J. Exp. Med. 164, 642 (1986) |
| 18 | E. coli. LPS 5014 | E. coli. LPS 5014, 0.5 mg/ml | Lipopolysaccharides (rough strains) from Escherichia coli J5 (Rc mutant) | Sigma-Aldrich | This report |
| 19 | S. dysenterine type 1 | S. dysenterine type I O-SP, 0.5 mg/ml | Shigella dysenteriae Type 1 O-specific polysaccharide | From Drs. John Robbins and Rachel Schneerson (NICHD, NIH) | Pozsgay, et al., Proc Natl Acad Sci USA 104:14478–14482 (2007) |
| 20 | S.typhi LPS | S.typhi LPS7261, 0.5 mg/ml | Lipopolysaccharides from Salmonella enterica serotype typhimurium L7261 | Sigma-Aldrich | This report |
| 21 | Cardiolipin/PTC_1/100 4 M | Cardiolipin/PTC, 0.02 mg/2 mg/ml, 4°C, 4 Months | Cardiolipin (C1649) | Sigma Chemical Co., St. Louis, MO | This report |
| 22 | PTC_D1 | PTC 2.0 mg/ml, 4°C, 24 h | L-α-Phosphatidylcholine (Egg, Chicken) | Avanti Polar lipids, Alabaster, AL | This report |

| Antigen ID# | Antigen name | Antgen preparations* | Description | Source | References |
|---|---|---|---|---|---|
| 23 | PTC_4 M | PTC 2.0 mg/ml, 4°C, 4 Months | L-α-Phosphatidylcholine (Egg, Chicken) | Avanti Polar lipids, Alabaster, AL | This report |
| 24 | PTC_12 M | PTC 2.0 mg/ml, 4°C, 12 Months | L-α-Phosphatidylcholine (Egg, Chicken) | Avanti Polar lipids, Alabaster, AL | This report |
| 25 | PTC_14 M | PTC 2.0 mg/ml, 4°C, 14 Months | L-α-Phosphatidylcholine (Egg, Chicken) | Avanti Polar lipids, Alabaster, AL | This report |
| 26 | Ganglioside/PTC_1/10 | Ganglioside/PTC, 0.2 mg/2 mg/ml, 4°C, 24 h | Total Ganglioside Extract (Brain, Porcine-Ammnium Salt) | Avanti Polar lipids, Alabaster, AL | This report |
| 27 | Erythrosphingosine/PTC_1/10 | Erythrosphingosine/PTC, 0.2 mg/2.0 mg/ml, 4°C, 24 h | D-erythro-Sphingosine (Egg, Chicken) | Avanti Polar lipids, Alabaster, AL | This report |
| 28 | Phytosphingosine/PTC_1/10 | Phytosphingosine/PTC, 0.2 mg/2.0 mg/ml, 4°C, 24 h | Phytosphingosine 4-Hydroxysphinganine (Saccharomyces cervisiae) | Avanti Polar lipids, Alabaster, AL | This report |
| 29 | Glucocerebroside/PTC_1/10 | Glucocerebroside/PTC, 0.2 mg/2 mg/ml, 4°C, 24 h | Glucocerebrosides (Soy, 98%) | Avanti Polar lipids, Alabaster, AL | This report |
| 30 | Sulfatide/PTC_1/10 | Sulfatide/PTC, 0.2 mg/2.0 mg/ml, 4°C, 24 h | Sufatides (Cerebroside sulfates) (Brain, Porcine) | Avanti Polar lipids, Alabaster, AL | This report |
| 31 | Ceremide/PTC_1/10 | Ceremide/PTC, 0.2 mg/2.0 mg/ml, 4°C, 24 h | Ceramide (Brain, Porcine) | Avanti Polar lipids, Alabaster, AL | This report |
| 32 | Cerebroside/PTC_1/10 | Cerebroside/PTC, 0.2 mg/2.0 mg/ml, 4°C, 24 h | Total Cerebrosides (Brain, Porcine) | Avanti Polar lipids, Alabaster, AL | This report |
| 33 | DMPS/PTC_1/10 | DMPS/PTC, 0.2 mg/2.0 mg/ml, 4°C, 24 h | 1,2-Dimyristoyl-sn-Glycero—3—[phospho-L—serine](Sodium Salt) (DMPS) | Avanti Polar lipids, Alabaster, AL | This report |
| 34 | Cardiolipin/PTC-1/20 D1 | Cardiolipin/PTC, 0.1 mg/2 mg/ml, 4°C, 24 h | Cardiolipin-Disodium Salt (heart, bovin) | Sigma Chemical Co., St. Louis, MO | This report |
| 35 | Cardiolipin/PTC-1/5_D1 | Cardiolipin/PTC, 0.4 mg/2 mg/ml, 4°C, 24 h | Cardiolipin-Disodium Salt (heart, bovin) | Sigma Chemical Co., St. Louis, MO | This report |
| 36 | Cardiolipin/PTC-1/20 4 M | Cardiolipin/PTC, 0.1 mg/2 mg/ml, 4°C, 4 Months | Cardiolipin-Disodium Salt (heart, bovin) | Sigma Chemical Co., St. Louis, MO | This report |

| Antigen ID# | Antigen name | Antgen preparations* | Description | Source | References |
|---|---|---|---|---|---|
| 37 | Cardiolipin/PTC-1/5 4 M | Cardiolipin/PTC, 0.4 mg/2 mg/ml, 4°C, 4 Months | Cardiolipin-Disodium Salt (heart, bovin) | Sigma Chemical Co., St. Louis, MO | This report |
| 38 | GM1/PTC_1/100 | GM1/PTC, 0.02 mg/2 mg/ml, 4°C, 24 h | GM1 Ganglioside-Sodium Salt (Brain, Ovine) | Avanti Polar lipids, Alabaster, AL | This report |
| 39 | GM1/PTC_1/10 | GM1/PTC, 0.2 mg/2 mg/ml, 4°C, 14 Months | GM1 Ganglioside-Sodium Salt (Brain, Ovine) | Avanti Polar lipids, Alabaster, AL | This report |
| 40 | αGal-T2/PTC_1/20 | Galαl,3Galβ1-* HDPE/PTC, 0.04 mg/2 mg/ml, 4°C, 12 Months | Galαl,3Galβ1-HDPE (αGal-terminal disaccharides) | V-LABS, INC, Louisiana, US | This report |
| 41 | Lactosamine/PTC | Galβl,4GlcNACβ1-HDPE/PTC, 4°C, 12 Months | Galβl,4GlcNACβ1-HDPE (Type II chain unit) | V-LABS, INC, Louisiana, US | This report |
| 42 | αGal-T3/PTC | Galαl,3Galβl, 4GlcNACβ1-HDPE/ PTC, 4°C, 12 Months | Galαl,3Galβl,4GlcNACβl-(αGal-terminal disaccharides)-HDPE | V-LABS, INC, Louisiana, US | This report |
| 43 | Ceremide | Ceremide, 2.0 mg/ml | Ceramide (Brain, Porcine) | Avanti Polar lipids, Alabaster, AL | This report |
| 44 | Sulfatide | Sulfatide, 2.0 mg/ml | Sufatides (Cerebroside sulfates), (Brain, Porcine) | Avanti Polar lipids, Alabaster, AL | This report |
| 45 | Ganglioside | Ganglioside, 2.0 mg/ml | Total Ganglioside-Ammonium Salt, (Brain, Porcine) | Avanti Polar lipids, Alabaster, AL | This report |
| 46 | DIMPS | DIMPS, 2 mg/ml | 1,2-Dimyristoyl-sn-Glycero–3–[phospho-L–serine](Sodium Salt) (DMPS) | Avanti Polar lipids, Alabaster, AL | This report |
| 47 | MBP1–11 | MBP1–11, 1 mg/ml | A synthetic peptide of human myelin basic protein(MBP), N-terminal amino acid 1–11 | Present authors | Robinson et al., Nat. Med., 8:295–301 (2002) |
| 48 | hMBP | hMBP, 0.5 mg/ml in 10 mM HCl | Myelin Basic Protein, iodination grade (Brain, Human) | ACCURATE CHEMICAL & SCIENTIFIC CORPORATION, WESTBURY, NY | Robinson et al., Nat. Med., 8:295–301 (2002) |
| 49 | mMBP | mMBP, 0.5 mg/ml | Myelin Basic Protein (Brain, Murine) | ACCURATE CHEMICAL & SCIENTIFIC CORPORATION, WESTBURY, NY | Robinson et al., Nat. Med., 8:295–301 (2002) |

| Antigen ID# | Antigen name | Antgen preparations* | Description | Source | References |
|---|---|---|---|---|---|
| 50 | MOG | M0G, 1 mg/ml | Myelin Oligodendrocyte Glycoprotein (Brain, Human) | ACCURATE CHEMICAL & SCIENTIFIC CORPORATION, WESTBURY, NY | Robinson et al., Nat. Med., 8:295–301 (2002) |
| 51 | PLP139–150 | PLP139–150, 1 mg/ml | A synthetic peptide of human Myelin Proteolipid Protein (PLP), Amino acid residue 139–150 | Present authors | Robinson et al., Nat. Med., 8:295–301 (2002) |
| 52 | Man9-BSA | Man9-BSA | $(Man9GlcNAc2Asn)_n$-BSA | Present authors | Wang, et al., Drug Dev. Res. 74:65–80, (2013) |

* The antigen concentrations for initial microarray spotting were listed. The subsequent dilutions of each antigens were specified in Figures 1–3.

** HDPE: Neoglycolipids-1,2-di-O-hexadecyl-sn-glycero-3—phosphoethanolamine.

## TABLE 2

Patient Demographics and Clinical Characteristics for Cerebrospinal Fluid Samples

| Sample ID | Diagnosis* | Age | Gender |
|---|---|---|---|
| Group 1 | Multiple sclerosis (MS) (*n* = 11) | | |
| 01-119 | SPMS | 58 | M |
| 01-168 | RRMS | 42 | F |
| 01-182 | RRMS | 27 | F |
| 01-188 | RRMS | 26 | F |
| 01-189 | RRMS | 56 | F |
| 01-190 | RRMS | 26 | F |
| 02-012 | RRMS | 33 | F |
| 02-013 | RRMS | 31 | F |
| 02-014** | RRMS | 37 | F |
| 02-015** | RRMS | 32 | F |
| 02-023 | RRMS | 45 | F |
| Group 2 | Other neurological disease (*n* = 9) | | |
| 01-180 | Tension headache | 35 | M |
| 01-181 | Vertigo | 36 | F |
| 01-184 | Tension headache | 58 | F |
| 01-183 | Vertigo | 58 | F |
| 01-185 | Vertigo | 51 | M |
| 02-001 | Slipped disc S1 | 30 | F |
| 02-010 | Spinal stenosis in cervical spine & chronic pain | 43 | F |
| 02-016 | Sensory symptoms | 20 | F |
| 02-019 | Vestibular neuritis | 36 | M |

* Diagnosis at the time of sampling.

** Immunomodulatory treatment being taken by the patient at the time of sampling.

SPMS, secondary progressive multiple sclerosis; RRMS, relapsing-remitting multiple sclerosis;